TOXICOLOGICAL SCIENCES **91(1)**, 159–165 (2006)
doi:10.1093/toxsci/kfj122
Advance Access publication January 27, 2006

Penetration of Intact Skin by Quantum Dots with Diverse Physicochemical Properties

Jessica P. Ryman-Rasmussen, Jim E. Riviere, and Nancy A. Monteiro-Riviere[1]

Center for Chemical Toxicology Research and Pharmacokinetics, College of Veterinary Medicine, North Carolina State University, Raleigh, North Carolina 27606

Received November 22, 2005; accepted January 13, 2006

Skin is the largest organ of the body and is a potential route of exposure to engineered nanomaterials, but the permeability of the skin to these nanomaterials is unknown. We selected commercially available quantum dots (QD) of two core/shell sizes and shapes and three different surface coatings to determine if QD could penetrate intact skin in a size- or coating-dependent manner. Spherical 4.6 nm core/shell diameter QD 565 and ellipsoid 12 nm (major axis) by 6 nm (minor axis) core/shell diameter QD 655 with neutral (polyethylene glycol), anionic (carboxylic acids) or cationic (polyethylene glycol-amine) coatings were topically applied to porcine skin in flow-through diffusion cells at an occupationally relevant dose for 8 h and 24 h. Confocal microscopy revealed that spherical QD 565 of each surface coating penetrated the stratum corneum and localized within the epidermal and dermal layers by 8 h. Similarly, polyethylene glycol– and polyethylene glycol-amine–coated ellipsoid QD 655 localized within the epidermal layers by 8 h. No penetration of carboxylic acid–coated QD 655 was evident until 24 h, at which time localization in the epidermal layers was observed. This study showed that quantum dots of different sizes, shapes, and surface coatings can penetrate intact skin at an occupationally relevant dose within the span of an average-length work day. These results suggest that skin is surprisingly permeable to nanomaterials with diverse physicochemical properties and may serve as a portal of entry for localized, and possibly systemic, exposure of humans to QD and other engineered nanoscale materials.

Key Words: **quantum dots; semiconductor nanocrystals; skin; nanomaterials; nanotoxicology.**

INTRODUCTION

Semiconductor nanocrystals, or quantum dots (QD) have great potential for use as diagnostic and imaging agents in biomedicine and as semiconductors in the electronics industry. The skin is the largest organ of the body, and it is a potential route of exposure to QD for producers and consumers, but the permeability of the skin to QD is unknown.

Quantum dots are heterogeneous nanoparticles that consist of a colloidal core surrounded by one or more surface coatings. Surface coatings in one or more layers are frequently applied to customize QDs to specific applications, such as the use of hydrophilic coatings to increase solubility in a biologically compatible medium, coatings (or ''shells'') that reduce leaching of metals from the core (Derfus *et al.*, 2004), and reactive surface groups that facilitate conjugation to therapeutic and diagnostic macromolecules, receptor ligands, or antibodies (Michalet *et al.*, 2005). Unlike other engineered nanostructures, QD are easily detected because of their unusually intense and photostable fluorescence. They are commercially available in various sizes and shapes with diverse surface coatings. Thus, QD are readily accessible tools by which the nanotoxicologist can determine the permeability of skin to engineered nanostructures with differing physicochemical properties, the results of which are of both practical and heuristic importance.

Flow-through diffusion cells are an established *in vitro* model for measuring the permeability of skin to penetrants (Bronaugh, 2000, 2006). Porcine skin is widely used for skin absorption studies because it is anatomically, physiologically, and biochemically similar to human skin (Monteiro-Riviere, 1991; Monteiro-Riviere and Riviere, 1996; Monteiro-Riviere and Stromberg, 1985; Simon and Maibach, 2000). Dermatomed skin, uniform in thickness, is individually mounted in flow-through cells such that the surface is exposed to air while the underlying dermis is perfused at a constant flow rate with nutritive medium at physiological temperature and pH (Bronaugh and Stewart, 1985). The penetrant concentration can be monitored in the perfusate, from which the rate and extent of skin absorption can be determined.

The goal of this study was to determine if QD could penetrate intact skin at an occupationally relevant dose within 8 h, the time span of an average-length work day. We selected commercially available, soluble quantum dots (QD) of two core/shell sizes and shapes, spherical QD 565 with a 4.6 nm core/shell diameter and ellipsoid QD 655 that measure 12 nm (major axis) × 6 nm (minor axis) in size. Quantum dots 565

[1] To whom correspondence should be addressed at Center for Chemical Toxicology Research and Pharmacokinetics, North Carolina State University, 4700 Hillsborough Street, Raleigh, NC 27606. Fax: 919–513–6358. E-mail: Nancy_Monteiro@ncsu.edu; CCTRP Homepage: http://cctrp.ncsu.edu.

and 655 were obtained with neutral (polyethylene glycol), anionic (carboxylic acids), or cationic (polyethylene glycol-amine) coatings. Quantum dots were topically applied to porcine skin mounted in flow-through diffusion cells, and confocal microscopy was used to reveal QD localization in the skin layers. The results of this study indicate that the skin is surprisingly permeable to QD with diverse physicochemical properties, which has important implications for nanomaterials risk assessment.

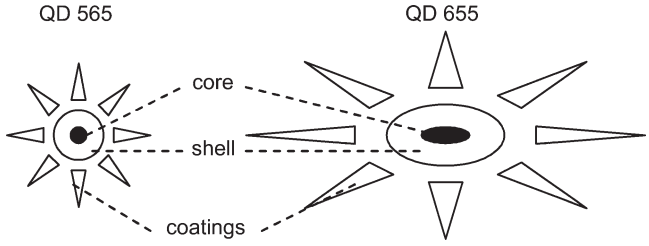

FIG. 1. Schematic of QD composition.

MATERIALS AND METHODS

Quantum dots. Quantum dots spherical or ellipsoid in shape of different core/shell sizes were obtained from Quantum Dot Corporation/Invitrogen (Hayward, CA). Quantum dots with emission maxima at 565 nm and 655 nm were chosen based on availability of all three surface coatings in each size and shape and minimal fluorophore overlap when using conventional emission filter sets. A schematic of QD 565 and QD 655 composition is provided in Figure 1. Quantum dots with fluorescence emission maxima at 565 nm (QD 565) are spherical, with a core/shell diameter of 4.6 nm. Quantum dots with emission maxima at 655 nm (QD 655) are ellipsoid, with a core/shell diameter 6 nm (minor axis) × 12 nm (major axis) (Quantum Dot Corporation, 2005). Each size was obtained with three different coatings expected to be uncharged (polyethylene glycol, PEG), negatively charged (carboxylic acid), or positively charged (PEG-amine) in the provided buffers and at physiological pH, based on approximate pKa values of ionizable groups (primary aliphatic amine pKa > 9, carboxylic acid pKA < 5, PEG ionization negligible). These were sold as Qtracker® Non-targeted Quantum Dots (PEG) or Qdot® ITK™ Carboxyl or Amino (PEG-amine) Quantum Dots, respectively. These hydrophilic coatings increase QD size severalfold in aqueous solution as a result of solvation effects, an increase that is reflected in the hydrodynamic diameter. The hydrodynamic diameters in the manufacturer's provided buffers of spherical QD 565 were 35 nm (PEG), 14 nm (COOH), and 15 nm (NH_2) and of ellipsoid QD 655 were 45 nm (PEG), 18 nm (COOH), and 20 nm (NH_2) along the major axis (Quantum Dot Corporation, 2005). The physicochemical properties (core/shell size, hydrodynamic diameter, shape, and surface charge) of all QD are summarized in Table 1. Quantum dots were supplied at concentrations ranging from 2 μM to 8.7 μM in a 50 mM borate buffer of pH 9.0 (carboxylic acid–coated QD) or pH 8.3 (all others) and were vortexed for 1 min and diluted to working concentrations in the appropriate borate buffer immediately before experimental use.

Animals. The care and experimental use of pigs used in this study were in accordance with animal care and use guidelines approved by North Carolina State University, where these experiments were conducted. Female Yorkshire weanling pigs 13–18 kg in mass were singly housed and allowed free access to food and water. On the days of the experiment, the pigs were sedated with an intramuscular injection of telazol (6 mg/kg), ketamine (3 mg/kg), and xylazine (3 mg/kg) and sacrificed by intravenous injection of 100 mg/kg Euthasol® (Delmarva Laboratories, Inc., Midlothian, VA). A 400-μm-thick area of skin on the back of the pig was removed as previously described (Chang and Riviere, 1991).

QD dose and duration. A dose of 62.5 pmoles per cm^2 was selected and was applied to flow-through diffusion cells for 8 h or 24 h. This corresponds to an exposure scenario in which one 40 μl drop of QD at 1 μM concentration (a 2–9-fold dilution of the concentration at which QD are supplied) is applied to 0.64 cm^2 of skin and remains during the course of a work day or overnight. During this time, a fraction of the dose dries on the skin surface and is not available for absorption.

Flow-through diffusion cells. The experimental protocol routinely used by our laboratory was adapted from previously published procedures (Bronaugh and Stewart, 1985; Chang and Riviere, 1991). Freshly dermatomed porcine skin was removed with a 20-mm diameter metal punch and mounted in flow-through diffusion cells with an exposed treatment area of 0.64 cm^2. Diffusion cells were equilibrated in perfusate (1.2 mM KH_2PO_4, 32.7 mM $NaHCO_3$, 2.5 mM $CaCl_2$, 4.8 mM KCl, 1.2 mM $MgSO_4$*$7H_2O$, 118 mM NaCl, 1200 mg/l D-glucose, 4.5% BSA, 5 U/ml heparin, 30 μg/ml amikacin, and 12.5 U/ml penicillin G) at 2 ml/h for 30 min prior to loading with QD or borate buffer controls. Diffusion cells were run at a flow rate of 2 ml/h for 8 h or 24 h, with perfusate collected for fluorescence detection each hour for the first 8 h and every 4 h thereafter (for 24-h experiments). At the end of the experiments, skin was immediately frozen at −20°C. Skin was sectioned at 20 μm on a cryostat prior to imaging. A total of three diffusion cells were run for each buffer control (50 mM borate pH 8.3 or 9.0) and for each QD type and exposure time. Each QD or vehicle was tested on two different pigs during experiments performed on 2 different days.

Fluorescence measurements of perfusate. A 200-μl aliquot of perfusate sample from each 1 h fraction was transferred to black 96-well plates with microclear bottoms (Corning/Costar USA) and read on a tunable Molecular Dynamics Gemini EM™. The excitation window was set at 360 nm for both QD 565 and QD 655 and emission widow set at 565 nm with a 550 nm cutoff (QD 565) or 655 nm with a 630 nm cutoff (QD 655). Fluorescence was compared to background values (perfusate without QD).

TABLE 1
Summary of the Physicochemical Properties of QD Used in This Study

QD type (565 or 655) and coating	Core/shell shape	Core/shell diameter (nm)	Hydrodynamic diameter (nm)	Expected surface charge
QD 565-PEG	Spherical	4.6	35	Neutral/uncharged
QD 565-PEG-amine	Spherical	4.6	15	Positive
QD 565-carboxylic acid	Spherical	4.6	14	Negative
QD 655-PEG	Ellipsoid	6 nm (minor axis), 12 nm (major axis)	45	Neutral/uncharged
QD 655-PEG-amine	Ellipsoid	6 nm (minor axis), 12 nm (major axis)	20	Positive
QD 655-carboxylic acid	Ellipsoid	6 nm (minor axis), 12 nm (major axis)	18	Negative

Confocal microscopy. Quantum dots were imaged in the skin layers using a Nikon C1 confocal laser scanner connected to a Nikon Eclipse 2000E inverted fluorescence microscope with a 40× Plan Fluor ELWD (dry) objective (0.60 NA). Quantum dots were excited with a 488 nm Ar laser line with filter-based emission channels of 565–615 nm (QD 565) and 630 nm and above (QD 655). Confocal-differential interference contrast microscopy (confocal-DIC) images of the skin layers were obtained by excitation with a 633 nm HeNe laser line. Images were captured using Nikon EZ-C1 software (version 2.01.152). The full thickness (approximately 20 μm) of all skin sections were scanned in 1-μm steps prior to image acquisition. Only the interior images (ca 10 μm from either surface) were chosen to avoid the possibility of any surface QD contamination from the sectioning knife. All imaging data are representative of each of three individual diffusion cell experiments.

RESULTS

Fluorescence Measurements of Perfusate

We were unable to detect QD in the perfusate by this method, which had detection limits of 0.5–1.0 nM for QD 565 and 0.25–0.5 nM for QD 655. This detection limit corresponds to approximately 0.5% of the applied dose.

Confocal Microscopy of Vehicle-Treated Controls

The morphology of the skin after treatment for 8 h with buffer similar to that in which the QD are supplied (50 mM borate pH 9.0) is shown in Figure 2A. The intact stratum corneum, or outermost layer of the skin can be seen, followed by the epidermal layers and the dermis. Tissue autofluorescence under our experimental conditions was negligible.

Confocal Microscopy of QD 565-Treated Skin

Spherical QD 565 of all three surface coatings penetrated the skin by 8 h (Fig. 3). A thick, compact, and intact stratum corneum was evident in all treatments (Fig. 3, top row, DIC images), which provides macroscopic evidence that penetration was not due to skin abrasion. Polyethylene glycol and carboxylic acid–coated QD 565 were localized primarily in the epidermal layers by 8 h, whereas QD 565 coated with PEG-amines were localized primarily in the dermis (Fig. 3, middle row, green). In all three cases, the fluorescence intensity maps (see Fig. 3, bottom row and Fig. 2B for intensity map) showed a clear concentration gradient of QD 565 localization, ranging from high in the stratum corneum (white/red) to low (blue) after penetration into the underlying epidermal and dermal layers.

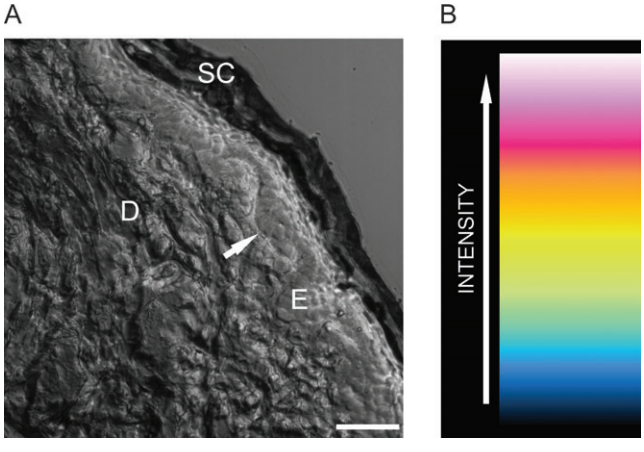

FIG. 2. A. Confocal-DIC image of skin treated with buffer only for 8 h (control). The stratum cornuem (SC), the outermost layer of the skin, the epidermis (E), and dermis (D) are clearly visible. The arrow indicates the epidermal/dermal junction. The scale bar (lower right corner) is 50 μm. B. Fluorescence intensity scale from low (blue) to high (red/white).

Confocal Microscopy of QD 655-Treated Skin

The ellipsoid QD 655 demonstrated differences in skin localization compared to the spherical QD 565 with similar coatings (Fig. 4A). Quantum dots 655 coated with PEG and PEG-amines were localized primarily within the epidermal layers after 8 h (Fig. 4A, middle row, red). A thick, compact, and intact stratum corneum was evident (Fig. 4A, top row, DIC images), indicating that the penetration of PEG and PEG-amine QD 655 occurred through normal and not abraded skin. Carboxylic acid-coated QD 655 did not penetrate through the stratum corneum into the underlying epidermal or dermal layers by 8 h (Fig. 4A, middle row, red). However, confocal microscopy showed that carboxylic acid-coated QD 655 were localized in the epidermal layers by 24 h (Fig. 4B, middle row, red). Skin penetration of coated QD 655 followed a concentration gradient in all cases (Fig. 4 A and B, bottom), ranging from high concentration in the stratum corneum (white/red) to low concentration in the epidermal layers.

DISCUSSION

The skin is a potential route of exposure to quantum dots and other engineered nanomaterials for both producers and consumers. This study employed porcine skin flow-through diffusion cells in conjunction with confocal microscopy to show that quantum dots of different sizes, shapes, and surface coatings can penetrate normal skin and become localized within the skin layers by 8 h. This result is important for nanomaterials risk assessment, because it suggests that occupationally relevant concentrations of QD and other nanomaterials with diverse physicochemical properties can penetrate intact skin.

We measured the fluorescence of the perfusate from the flow-through diffusion cells at 1-h intervals from 1 h to 24 h after topical application of QD 565 and 655 coated with PEG, PEG-amines, or carboxylic acids with the intention of determining the pharmacokinetics of QD penetration. Our detection limits did not allow detection of QD in perfusate above background levels. There are several explanations unrelated to detection limits that could account for an apparent lack of QD

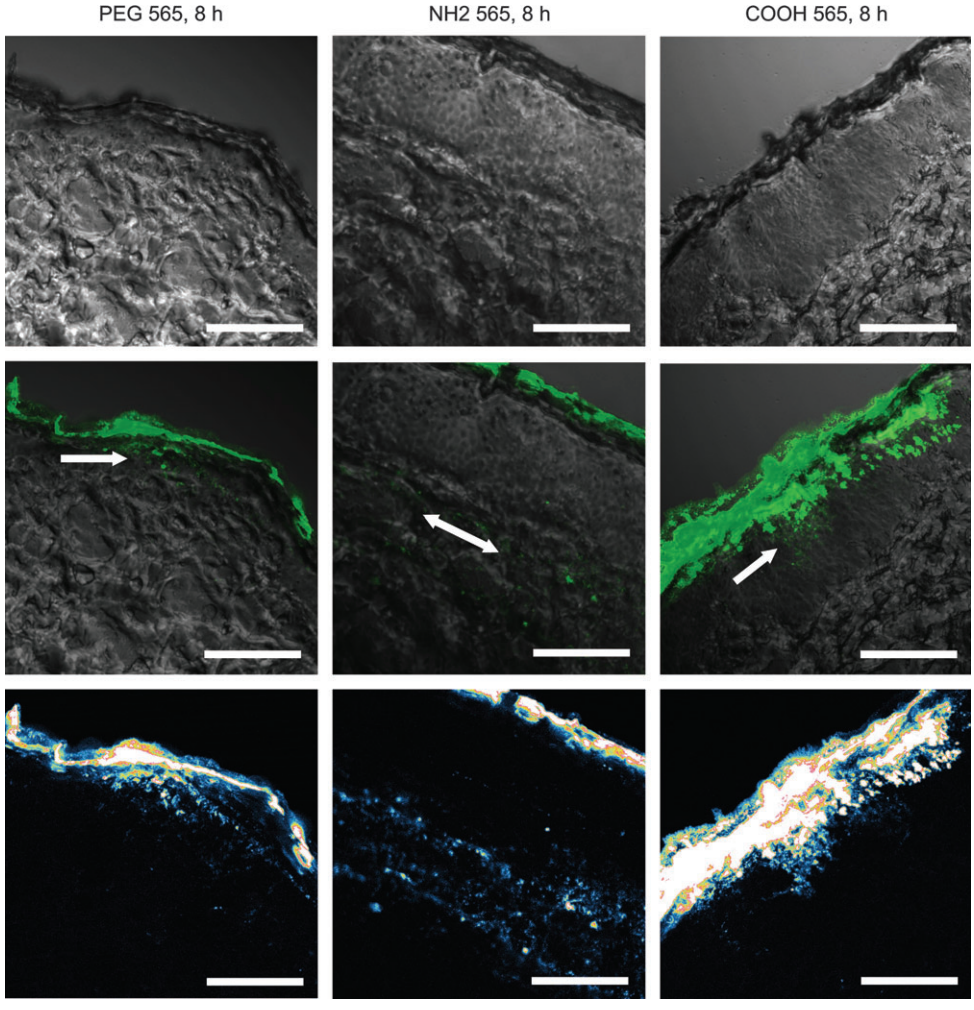

FIG. 3. Confocal scanning microscopy of skin treated for 8 h with PEG, PEG-amine (NH2), or carboxylic acid (COOH)-coated QD 565. Coatings are noted at the top of each column. Top row: confocal-DIC channel only allows an unobstructed view of the skin layers. Middle row: confocal-DIC overlay with the QD fluorescence channel (green) shows QD localization within the skin layers. Arrows indicate QD localization in the epidermis or dermis. Bottom row: fluorescence intensity scan of QD emission. Quantum dots 565 are localized in the epidermal (PEG and COOH coatings) or dermal (NH2 coating) layers by 8 h. All scale bars (lower right corners) are 50 μm.

fluorescence in the perfusate. First, a considerable fraction of the applied dose dried on the skin surface and was not available for penetration. Second, each fraction would have to contain at least 5% of the applied dose for significant fluorescence to be detectable in our assay, which had a detection limit of 0.5% of the applied dose. Third, it would not be unusual for elution of absorbed QD from the skin to span several hours, which would require absorption of a fairly large percentage of the applied dose (10% or greater). Fourth, compounds that penetrate the stratum corneum layer may be retained in the epidermal or dermal skin layers, which would further delay (or preclude) elution in the perfusate. Finally, dermatomed skin in diffusion cells lacks an intact vasculature. This requires QD to diffuse through the entire thickness of the dermis before they reach the perfusate. Extensive vascular networks *in vivo* greatly decrease the dermal path length QD have to travel for access to the bloodstream. For this reason, perfusate analysis alone is insufficient to determine if QD can penetrate skin, and it likely underestimates absorption. Confocal microscopy provided an alternative means of analysis and allowed visualization of QD localization within skin layers, which was evident by 8 h in all but one case.

Polyethylene glycol–coated QD 565 and 655 penetrated through the intact stratum corneum barrier and were localized primarily in the epidermal layers by 8 h. Previously, polymeric nanoparticles comprised of a PEG-containing block copolymer 40 nm in size have been found to penetrate to the epidermis when applied to hairless guinea pig skin by 12 h (Shim *et al.*, 2004). This result is consistent with the present study, because spherical, PEG-coated QD 565 and ellipsoid PEG-coated QD 655 are in this size range, with hydrodynamic diameters of 35 nm and 45 nm (major axis), respectively (Quantum Dot Corporation, personal communication, 2005). The fluorescence intensity maps of PEG-coated QD 565 and 655 penetration

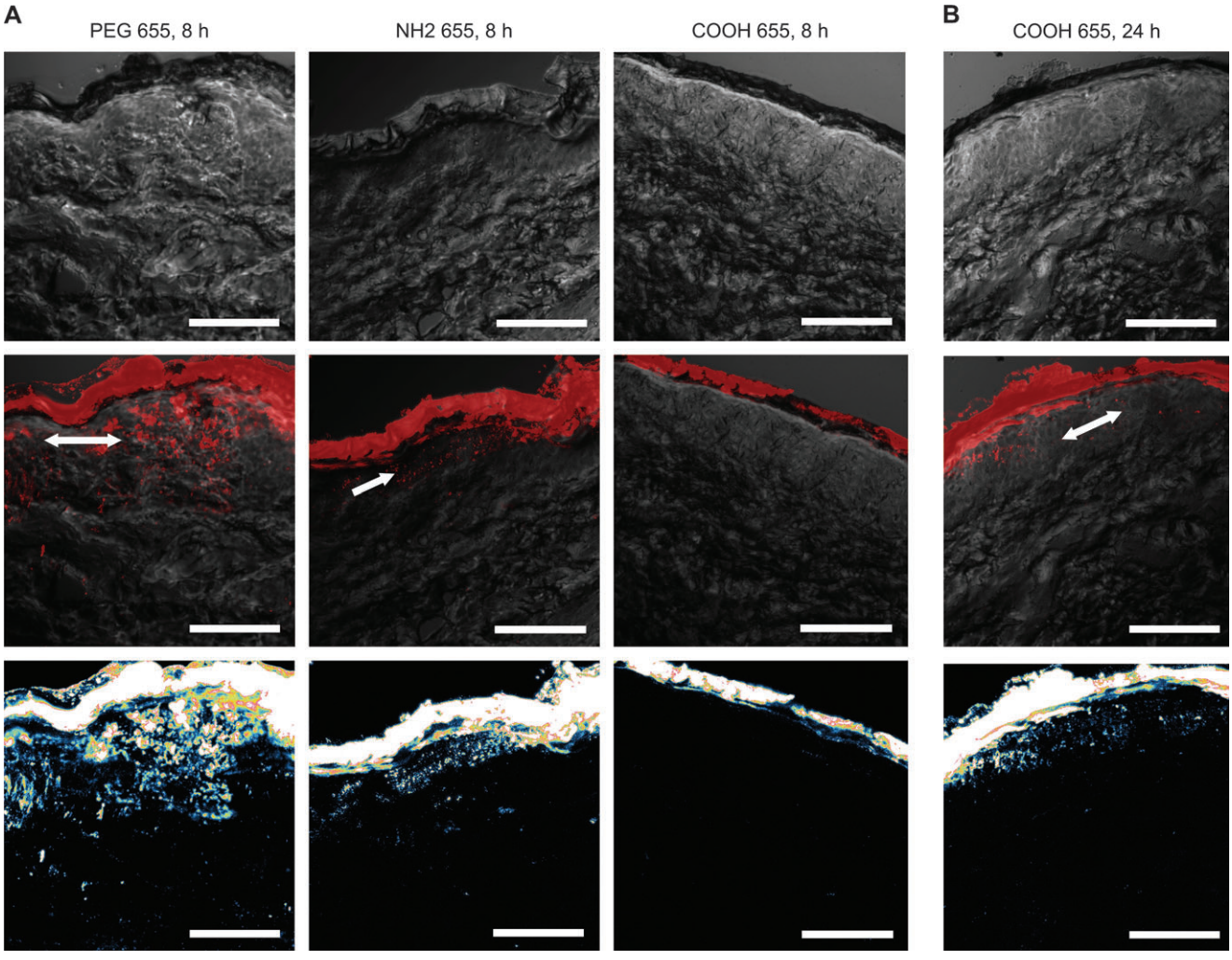

FIG. 4. A. Confocal scanning microscopy of skin treated for 8 h with PEG, PEG-amine (NH2), or carboxylic acid (COOH)-coated QD 655. Coatings are noted at the top of each column. Top row: confocal-DIC channel only allows an unobstructed view of the skin layers. Middle row: confocal-DIC overlay with the QD fluorescence channel (red) shows QD localization within skin layers. Arrows indicate QD localization in the epidermis. Last row: fluorescence intensity scan of QD emission. Quantum dots 655 coated with PEG or NH2 are localized in the epidermis, whereas no carboxylic acid-coated QD 655 penetrate the stratum corneum by 8 h. B. Confocal scanning microscopy of skin treated for 24 h showed carboxylic acid-coated QD 655 in the epidermis (middle, as indicated by arrow). The top image shows an obstructed view of the skin layers by confocal-DIC and the bottom image shows fluorescence intensity in the QD 655 emission channel. All scale bars in panels A and B (lower right corners) are 50 μm.

through the stratum corneum into the epidermal layers showed a clear concentration gradient in both cases. This pattern is most consistent with a passive diffusion mechanism of penetration.

Quantum dots 565 and 655 coated with PEG-amines also penetrated through the epidermis and localized within the epidermal (QD 655) and dermal (QD 565) layers by 8 h. Our observation of QD 565 localization in the dermal layers by 8 h was particularly impressive, given the thickness of the epidermis. Such penetration of QD into the richly vascularized dermis could facilitate systemic QD absorption. Again, the lack of an intact vasculature in dermatomed skin is of particular relevance. Quantum dots would likely traverse a shorter path length of the dermis *in vivo* for bloodstream access, depending upon the extent of local vascularization (Monteiro-Riviere *et al.*, 1993). For this reason, evidence of dermal penetration in a diffusion cell model should be of concern, regardless of the dermal depth observed *in vitro*. Fluorescence intensity maps of PEG-amine–coated QD 565 and 655 penetration are also consistent with a passive diffusion mechanism. The smaller hydrodynamic diameter of PEG-amine–coated QD 565 (15 nm) relative to PEG-coated QD 565 (35 nm) may partially explain the deeper penetration of PEG-amine QD 565 by 8 h (Quantum Dot Corporation, personal communication, 2005). However, PEG-amine–coated QD 655 with a hydrodynamic diameter of 20 nm primarily localized in the epidermal layers by 8 h. This was similar to results obtained from PEG-coated QD 655, which have a hydrodynamic size of 45 nm (Quantum Dot Corporation, personal communication, 2005). A 5-nm

difference in hydrodynamic size is probably not sufficient to explain the differences in penetration depths between QD 565 and 655 with PEG-amine coatings by 8 h. QD 565 and QD 655 do differ in shape, however, which may contribute to these differences in penetration depth.

The most surprising finding of this study was that carboxylic acid–coated QD 565 penetrated the stratum corenum and localized within the epidermal layers by 8 h, whereas QD 655 was not observed in the epidermis until 24 h after topical application. This result is especially intriguing when one considers that carboxylic acid–coated QD 565 and 655 have similar hydrodynamic sizes of 14 nm and 18 nm, respectively (Quantum Dot Corporation, personal communication, 2005). The most apparent physicochemical difference between these QD is shape. Thus, it is tempting to speculate that spherical carboxylic acid–coated QD penetrate skin more rapidly than ellipsoid-shaped QD. Caution should be exercised, however, because a previous study demonstrated no penetration of the stratum corneum by carboxylate-modified polystyrene spheres 20 nm in size, although the exposure time in that study was only 2 h (Alvarez-Roman *et al.*, 2004). Fluorescence intensity maps of carboxylic acid-coated QD penetration by 8 h (QD 565) and by 24 h (QD 655) were also consistent with a passive diffusion mechanism of penetration.

Our observations that QD with diverse physicochemical properties (size, shape, and surface coating) penetrated the stratum corenum barrier and localized within the epidermal and dermal layers by 8 h in all but one case, that of carboxylic acid–coated QD 655, which penetrated by 24 h, was unexpected. This result contradicts conventional thought, which is that the skin barrier is impervious to materials and that abrasion or other mechanical stressors would be required for nanomaterial penetration (Oberdorster *et al.*, 2005; Tinkle *et al.*, 2003). A potential criticism of our study is that the vehicles used for QD dilution, 50 mM borate buffer pH 8.3 for PEG and PEG-amine–coated QD and 50 mM borate buffer pH 9.0 for carboxylic acid–coated QD, caused or greatly facilitated QD penetration by damaging the skin. Two lines of evidence indicate that these vehicles did not compromise barrier function. First, the DIC-confocal data showed an intact and compact stratum corneum and preservation of skin morphology in all cases. Second, carboxylic acid–coated QD 655 did not penetrate until 24 h after application. One would expect skin penetration by 8 h as for the other QD tested if QD penetration were caused or significantly enhanced by skin injury. Finally, the vehicles used in this study are of the same formulation and pH as the buffers in which QD are supplied. It is essential to the validity of any dermal exposure study that experiments be conducted using the same solvents in which human exposures occur. Thus, even though vehicle-mediated alterations in skin permeability cannot be completely ruled out, the penetration effects we report remain valid, because the dosing solutions are representative of QD as commercially supplied, but at twofold to fourfold lower concentration.

Our observations based on the fluorescence intensity maps, which indicated passive diffusion of QD across the stratum corneum for all QD tested, was unexpected. Studies by other investigators using 20-nm microspheres have shown preferential accumulation in follicular openings, which might indicate a preference for transappendageal routes of penetration for nano-sized particles via hair follicles (Alvarez-Roman *et al.*, 2004). No frank penetration of the stratum corneum was observed in that study, however. It is interesting that QD differing in shape, hydrodynamic size, and surface coatings that are neutral (PEG), anionic (carboxlic acid), or cationic (PEG-amine) apparently penetrated the stratum corneum by the same mechanism. The fluorescence intensity maps suggested a passive diffusion mechanism, most likely via an intercellular route of passage between adjacent corneocytes. Recently, our laboratory reported that the size of the intercellular space between porcine skin corenocytes is 19 nm (van der Merwe *et al.*, 2005). Carboxylic acid and PEG-amine–coated QD 565 and 655 QD have similar hydrodynamic sizes in the delivery vehicle (14–20 nm), which is compatible with the hypothesis that penetration occurs by diffusion between the intercellular spaces. Polytheylene glycol–coated QD 565 and 655 are substantially greater in hydrodynamic size in the delivery vehicle (35 nm and 45 nm, respectively), but they still penetrated the corneum, in apparent conflict with an intercellular mechanism of penetration. However, the lipid microenvironment of the intercellular space (Fartasch *et al.*, 1993) might be expected to decrease the hydrodynamic size of coated QD by decreasing QD solvation. Additionally, the size of the intercellular space is probably not static, as evidenced by the dramatic effect of hydration status on intercellular space size (Warner *et al.*, 2003). Regardless of the operative mechanism(s) of QD penetration, our findings indicate that skin is permeable to nanomaterials with diverse physicochemical properties. If true, skin would serve as portal of entry for occupational and consumer exposures to a diversity of engineered nanostructures.

At present, it is not known if skin penetration of QD would result in adverse effects. However, we have observed intracytoplasmic localization of multi-walled carbon nanotubes (MWCNT), accompanied by a decrease in cell viability and a significant release of the pro-inflammatory cytokine IL-8 in primary human epidermal keratinocytes (Monteiro-Riviere *et al.*, 2005). Other investigators have reported decreased viability, morphological changes, and oxidative stress after treatment with single-walled carbon nanotubes (SWCNT) in immortalized skin cells (Shvedova *et al.*, 2003). There are apparently conflicting reports of QD toxicity in the literature (Derfus *et al.*, 2004; Jaiswal *et al.*, 2003; Lovric *et al.*, 2005; Shiosahara *et al.*, 2004). This is not unusual, because these studies have been conducted with QD differing in core/shell composition and surface coatings and in different cell lines, none of which are representative of skin tissue or the QD tested in this study. Penetration of QD into the epidermal layers of the

skin could result in a localized skin response, such as inflammation or cytotoxicity. Penetration of QD through the epidermal layers into the richly vascularized dermis could provide access for systemic absorption.

This study indicates that exposure of intact skin to QD results in dermal penetration. This finding was surprising because it contradicts conventional thought, which is that the skin barrier is impervious to materials and that abrasion or mechanical stressors would be required for nanomaterial penetration (Oberdorster *et al.*, 2005; Tinkle *et al.*, 2003). This finding is of importance to risk assessment for exposures to nanoscale materials, because it indicates that the dermal route should not be overlooked. The permeability of skin to QD differing in size, shape, and surface coatings indicates that skin may be similarly permeable to QD of diverse physicochemical properties.

ACKNOWLEDGMENTS

We thank the personnel at the Center for Chemical Toxicology Research and Pharmacokinetics of North Carolina State University for their excellent technical assistance. This study was supported by the U. S. Environmental Protection Agency (USEPA)-STAR Program under grant no. RD83171501.

REFERENCES

Alvarez-Roman, R., Naik, A., Kalia, Y. N., Guy, R. H., and Fessi, H. (2004). Skin penetration and distribution of polymeric nanoparticles. *J. Control Release* **99,** 53–62.

Bronaugh, R. L. (2000). *In vitro* percutaneous absorption models. *Ann. N. Y. Acad. Sci.* **919,** 188–191.

Bronaugh, R. L. (2006). *In vitro* diffusion cell studies. In *Dermal Absorption Models in Toxicology and Pharmacology* (J. E. Riviere, Ed.), pp. 21–27. CRC Press, Taylor and Francis, Boca Raton, FL.

Bronaugh, R. L., and Stewart, R. F. (1985). Methods for *in vitro* percutaneous absorption studies IV: The flow-through diffusion cell. *J. Pharm. Sci.* **74,** 64–67.

Chang, S. K., and Riviere, J. E. (1991). Percutaneous absorption of parathion *in vitro* in porcine skin: effects of dose, temperature, humidity, and perfusate composition on absorptive flux. *Fundam. Appl. Toxicol.* **17,** 494–504.

Derfus, A. M., Chan, W. C. W., and Bhatia, S. (2004). Probing the cytotoxicity of semiconductor nanocrystals. *Nano Lett.* **4,** 11–18.

Fartasch, M., Bassukas, I. D., and Diepgen, T. L. (1993). Structural relationship between epidermal lipid lamellae, lamellar bodies and desmosomes in human epidermis: An ultrastructural study. *Br. J. Dermatol.* **128,** 1–9.

Jaiswal, J. K., Mattoussi, H., Mauro, J. M., and Simon, S. M. (2003). Long-term multiple color imaging of live cells using quantum dot bioconjugates. *Nat. Biotechnol.* **21,** 47–51.

Lovric, J., Bazzi, H. S., Cuie, Y., Fortin, G. R., Winnik, F. M., and Maysinger, D. (2005). Differences in subcellular distribution and toxicity of green and red emitting CdTe quantum dots. *J. Mol. Med.* **83,** 377–385.

Michalet, X., Pinaud, F. F., Bentolila, L. A., Tsay, J. M., Doose, S., Li, J. J., Sundaresan, G., Wu, A. M., Gambhir, S. S., and Weiss, S. (2005). Quantum dots for live cells, *in vivo* imaging, and diagnostics. *Science* **307,** 538–544.

Monteiro-Riviere, N. A. (1991). Comparative anatomy, physiology, and biochemistry of mammalian skin. In *Dermal and Ocular Toxicology Fundamentals and Methods* (D. W. Hobson, Ed.), pp. 3–71. CRC Press, Boca Raton, FL.

Monteiro-Riviere, N. A., Inman, A. O., Riviere, J. E., McNeill, S. C., and Francoeur, M. L. (1993). Topical penetration of piroxicam is dependent on the distribution of the local cutaneous vasculature. *Pharm. Res.* **10,** 1326–1331.

Monteiro-Riviere, N. A., Nemanich, R. J., Inman, A. O., Wang, Y. Y., and Riviere, J. E. (2005). Multi-walled carbon nanotube interactions with human epidermal keratinocytes. *Toxicol. Lett.* **155,** 377–384.

Monteiro-Riviere, N. A., and Riviere, J. E. (1996). The pig as a model for cutaneous pharmacoloy and toxicology research. In *Advances in Swine in Biomedical Research* (M. E. Tumbleson and L. B. Schook, Eds.), pp. 425–458. Plenum Press, New York.

Monteiro-Riviere, N. A., and Stromberg, M. W. (1985). Ultrastructure of the integument of the domestic pig (*Sus scrofa*) from one through fourteen weeks of age. *Anat. Histol. Embryol.* **14,** 97–115.

Oberdorster, G., Oberdorster, E., and Oberdorster, J. (2005). Nanotoxicology: An emerging discipline evolving from studies of ultrafine particles. *Environ. Health Perspect.* **113,** 823–839.

Shim, J., Seok, K. H., Park, W. S., Han, S. H., Kim, J., and Chang, I. S. (2004). Transdermal delivery of minoxidil with block copolymer nanoparticles. *J. Control Release* **97,** 477–484.

Shiosahara, A., Hoshino, A., Hanaki, K., Suzuki, K., and Yamamoto, K. (2004). On the cytotoxicity caused by quantum dots. *Microbiol. Immunol.* **48,** 669–675.

Shvedova, A. A., Castranova, V., Kisin, E. R., Schwegler-Berry, D., Murray, A. R., Gandelsman, V. Z., Maynard, A., and Baron, P. (2003). Exposure to carbon nanotube material: Assessment of nanotube cytotoxicity using human keratinocyte cells. *J. Toxicol. Environ. Health A* **66,** 1909–1926.

Simon, G. A., and Maibach, H. I. (2000). The pig as an experimental animal model of percutaneous permeation in man: Qualitative and quantitative observations—an overview. *Skin Pharmacol. Appl. Skin Physiol.* **13,** 229–234.

Tinkle, S. S., Antonini, J. M., Rich, B. A., Roberts, J. R., Salmen, R., DePree, K., and Adkins, E. J. (2003). Skin as a route of exposure and sensitization in chronic beryllium disease. *Environ. Health Perspect.* **111,** 1202–1208.

van der Merwe, M. D., Brooks, J. D., Gehring, R., Baynes, R. E., Monteiro-Riviere, N. A., and Riviere, J. E. (2005). A physiological-based pharmacokinetic model of organophosphate dermal absorption. *Toxicol. Sci.* **89,** 188–204.

Warner, R. R., Stone, K. J., and Boissy, Y. L. (2003). Hydration disrupts human stratum corneum ultrastructure. *J. Invest. Dermatol.* **120,** 275–284.